JOURNAL OF PETROLOGY | VOLUME 43 | NUMBER 7 | PAGES 1109–1119 | 2002

A Time Frame for Construction of the Kerguelen Plateau and Broken Ridge

ROBERT A. DUNCAN*

COLLEGE OF OCEANIC AND ATMOSPHERIC SCIENCES, OREGON STATE UNIVERSITY, CORVALLIS, OR 97331, USA

RECEIVED JUNE 29, 2001; REVISED TYPESCRIPT ACCEPTED JANUARY 24, 2002

A key element in achieving Ocean Drilling Program Leg 183 science objectives is determining the age of volcanism at different locations across the Kerguelen Plateau and Broken Ridge. This paper reports crystallization ages derived from ^{40}Ar–^{39}Ar incremental heating experiments, for whole rocks and feldspars separated from basement units recovered at Sites 1136, 1137, 1138, 1139, 1140, 1141 and 1142. The subaerial environment of eruption at most sites and the generally evolved, high K content of these lava flows contributed to precise and reproducible age determinations. Volcanic activity at southern Kerguelen Plateau Site 1136 occurred at 118–119 Ma; at Elan Bank Site 1137, 107–108 Ma; at central Kerguelen Plateau Site 1138, 100–101 Ma; at Skiff Bank Site 1139, 68–69 Ma; at northern Kerguelen Plateau Site 1140, 34–35 Ma; and at Broken Ridge Sites 1141 and 1142, 94–95 Ma. The new ages allow calculation of melt production rates through the ~120 Myr history of the Kerguelen plume, adjustments to plate reconstructions for the eastern Indian Ocean region in the hotspot reference frame, and assessment of proposed links between large igneous province (LIP) magmatism and environmental crises.

KEY WORDS: *large igneous provinces; ^{40}Ar–^{39}Ar geochronology; ocean plateaux*

INTRODUCTION

Ocean Drilling Program (ODP) Leg 183 addresses four first-order problems related to the characterization and quantification of igneous crustal production at the Kerguelen Plateau large igneous province (LIP) and its possible atmospheric and oceanographic effects during Cretaceous and Cenozoic time (Coffin *et al.*, 2000). Specific objectives are to:

(1) determine the chronology of the Kerguelen Plateau–Broken Ridge magmatism;

(2) constrain the time scale of melting processes, and post-melting magmatic evolution;

(3) evaluate the effects of LIP formation on the environment;

(4) identify and interpret relationships between LIP development and tectonism.

Radiometric ages contribute directly to objectives (1) and (2) by determining the timing and duration of magmatic activity, which allow production rates to be estimated (see Coffin *et al.*, 2002). The most significant question is, how much magma was erupted over what period? The answer can be quantified only with precise radiometric ages distributed widely across the province. Ages are important in assessing objective (3) by providing a temporal framework for linking magmatic events with abrupt or gradual environmental changes recorded in proximal or distal sediments, such as chemical anomalies (e.g. Sinton & Duncan, 1997) or biological crises (e.g. Erba, 1994). Post-emplacement tectonic events [objective (4)] may have produced synchronous volcanic activity (e.g. Broken Ridge rifting from the central Keguelen Plateau), which would become apparent through age determinations.

In the larger context of Indian Ocean volcanic and tectonic evolution, the Kerguelen Plateau is the oldest oceanic portion of the Kerguelen hotspot–mantle plume system, which later formed the Ninetyeast Ridge, Kerguelen Archipelago and the young Heard and McDonald Islands (Fig. 1). The timing of volcanic activity along all parts of this system is a critical element of plate reconstructions in the fixed hotspot reference frame (e.g. Royer & Coffin, 1992), and in assessing models of plume dynamics. For example, Richards *et al.* (1989) and

*Fax: +1-541-737-2064. E-mail: rduncan@oce.orst.edu

Campbell & Griffiths (1990) proposed that surfacing plume heads have produced high mantle melting rates and widespread contemporaneous volcanism at the onset of hotspot activity, whereas Kent *et al.* (1992) attributed a much more significant role to overlying lithosphere, in controlling the distribution of volcanism, prolonging the duration of activity, and modifying the melting rates at the hotspot.

This paper reports crystallization ages derived from ^{40}Ar–^{39}Ar incremental heating experiments, for whole rocks and feldspars separated from basement units recovered at Sites 1136, 1137, 1138, 1139, 1140, 1141 and 1142. Cooling units were identified from shipboard measurements and examination of core and thin sections. These have been described by Coffin *et al.* (2000). Samples are referenced by ODP convention, to site number, core and section number, and centimeter-interval (Table 1 and Fig. 2).

PREVIOUS RESULTS

Knowledge of the age distribution of terminal volcanic activity across the Kerguelen Plateau has been extremely limited. Biostratigraphic data come from analysis of lowermost sediments recovered during ODP Legs 119 and 120 (Barron *et al.*, 1989; Schlich *et al.*, 1989) and a few surface samples (Leclaire *et al.*, 1987; Frohlich & Wicquart, 1989). Previous radiometric dating of Kerguelen Plateau derives from a single dredged sample (~114 Ma, K–Ar age, Leclaire *et al.*, 1987), and cored samples from ODP drilling sites (Legs 119 and 120). ^{40}Ar–^{39}Ar ages from the latter range from 109 to 113 Ma at ODP Sites 738, 749 and 750 (Whitechurch *et al.*, 1992; Pringle *et al.*, 1997) for the southern Kerguelen Plateau, and a poorly constrained age of ~85 Ma from Site 747 in the central Kerguelen Plateau (Pringle *et al.*, 1997). The basal, flood basalt portion of the Kerguelen Archipelago, northern Kerguelen Plateau, was constructed at ~40–23 Ma, whereas intermittent, central volcanic activity has continued up to the present (Nicolaysen *et al.*, 2000). Heard and McDonald Islands are young, active volcanoes in the central Kerguelen Plateau (Barling *et al.*, 1994). Ages of prominent submarine volcanoes lying between Heard Island and the Kerguelen Archipelago are 10–14 Ma, based on preliminary K–Ar dating (Weis *et al.*, 2002). Ages from dredged rocks from Broken Ridge are ~62 and 83–88 Ma (Duncan, 1991); the older group's range encompasses the Site 747 age, which supports the idea that Broken Ridge joins the central Kerguelen Plateau in pre-rift reconstructions (Royer & Coffin, 1992).

GEOCHRONOLOGICAL METHODS

Radiometric determination of the crystallization ages of fine-grained volcanic rocks of basaltic composition is best accomplished with K–Ar methods, because of the ubiquitous distribution of K in bulk rocks and Ar-retentive minerals (primarily feldspar), the suitability of the decay constant for ^{40}K in this time frame, and the precision with which mass spectrometric measurements can be made. Conventional, total fusion K–Ar analyses, however, are plagued by several effects that can produce inaccurate results.

The first of these is loss of ^{40}Ar during and following low-temperature burial metamorphism (zeolite facies), surface weathering, and seafloor alteration. The secondary mineral phases, such as clays and zeolites, that replace primary igneous phases do not quantitatively retain ^{40}Ar, so measured ages are typically significantly less than crystallization ages. The second important disruption is the incorporation of a non-atmospheric source of Ar (excess) at the time of crystallization. This is mantle derived and is borne in undegassed magmas and minerals that begin to crystallize at depth in the crust, or under high hydrostatic pressures. Hence, such rocks may not start out with an atmospheric composition of Ar, and ages calculated under this assumption are older than the time of crystallization. The net result of these geological effects is to produce a range of K–Ar ages that are inaccurate and greatly exaggerate the true duration of magmatism, as a result of increased scatter in the age data.

The ^{40}Ar–^{39}Ar incremental heating method provides the capability of separating the contributions of primary igneous and secondary alteration phases to the total sample Ar composition, and identifying any initial, non-atmospheric Ar, if present. This is accomplished, after neutron irradiation to produce ^{39}Ar from ^{39}K, by step heating the sample and analyzing the composition of Ar released at each step (e.g. Dalrymple *et al.*, 1981; McDougall & Harrison, 1999). Crystallization ages are then interpreted from convergence of step ages toward a mid- to high-temperature 'plateau' age, and independently from the slope of collinear step compositions in Ar-isotope ratio plots, i.e. an isochron age. Irradiation-induced Ar recoil (^{39}Ar and ^{37}Ar) and Ar loss can be significant and must be evaluated for each sample.

Experiments were run for both whole-rock basalts and feldspars separated from basaltic and rhyolitic units described by Coffin *et al.* (2000). Samples were selected for dating on the basis of shipboard macroscopic and microscopic examination, compositional data and stratigraphic significance. Whole rocks were prepared in two ways: a 0·5–1 mm size fraction of chips from fresh slabbed pieces, or mini-cores cut from fresh interiors of large pieces. Feldspar separates were cleaned in nitric acid, then briefly in 6% HF, followed by ultrasonic washing, and finally hand-picked. Chips and feldspar samples were wrapped in Cu foil, labeled, and loaded in quartz vials, along with the whole-rock mini-cores. Samples were

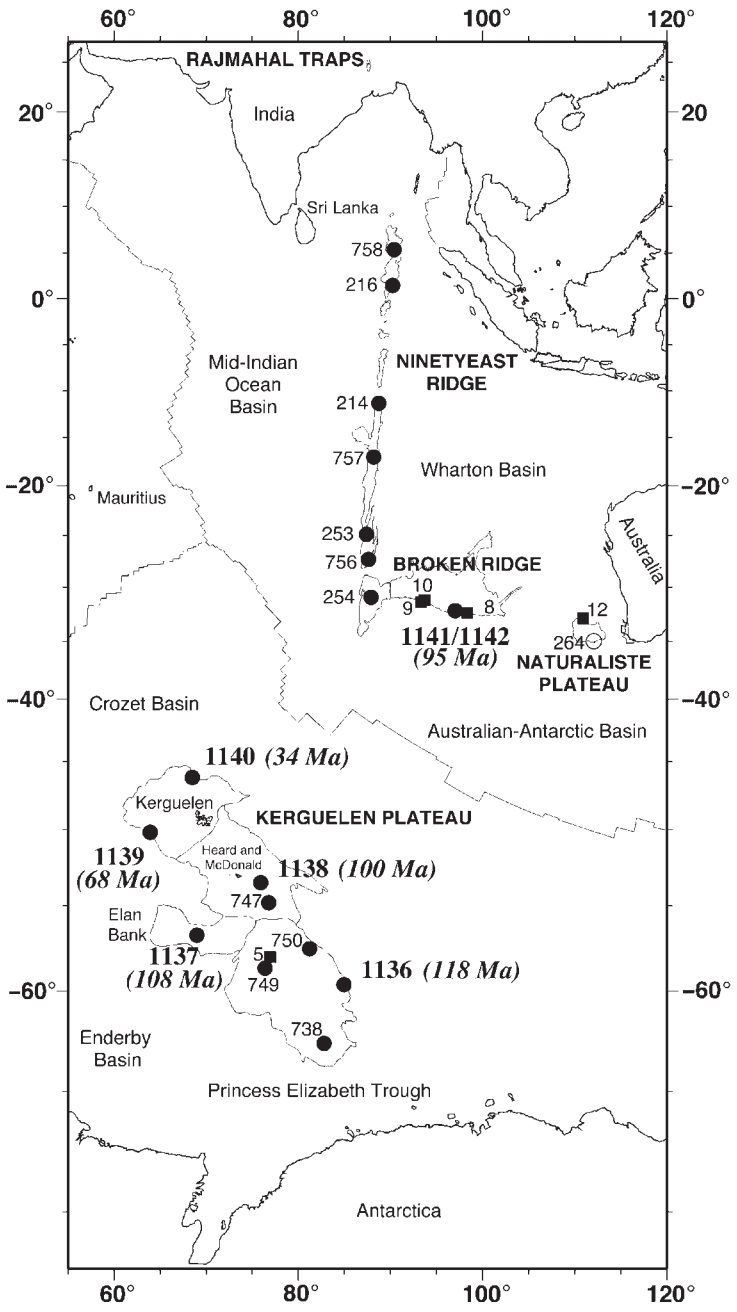

Fig. 1. Location map for sampling sites on the Kerguelen Plateau, Broken Ridge and related volcanic occurrences in the eastern Indian Ocean. Large, bold numbers are ODP Leg 183 drilling sites, with best mean basement ages (Ma) in italics; other, smaller numbers are previous ODP and Deep Sea Drilling Project drilling sites, and dredge locations. The Kerguelen Plateau is partitioned into proposed physiographic provinces (Coffin *et al.*, 2002) based on seismic reflection and gravity data.

interspaced with 10 mg aliquots of biotite monitor FCT-3 (28·04 ± 0·12 Ma, calibrated against Mmhb-1 hornblende at 523·5 Ma; Renne *et al.*, 1994). Quartz vials were evacuated, sealed in standard Al tubes and irradiated for 6–10 h at 1 MW power in the center ring of the TRIGA reactor at Oregon State University, Corvallis.

FCT-3 biotite was placed at multiple vertical positions along the 80 mm center vial, which provided neutron flux measurements ($\mathcal{J}$ values) that varied smoothly with a ~10% range. Horizontal gradients in $\mathcal{J}$ are known from previous experience to be <1%. $\mathcal{J}$ values for the sample positions were interpolated from a second-order

Table 1: Incremental heating ages for whole rocks and feldspars from Ocean Drilling Program Leg 183, Kerguelen Plateau and Broken Ridge

Sample	Material	Total gas age (Ma)	±2 SD	%^{39}Ar	Plateau age (Ma)	±2 SD	Steps used	MSWD	Isochron age (Ma)	±2 SD	MSWD	^{40}Ar/^{36}Ar (initial)	±2 SD
Hole 1136A													
16R1, 84–89	plagioclase	121·16	2·49	97·58	118·99	2·11	7 of 8	1·11	117·32	2·58	0·38	323	27
18R2, 83–94	plagioclase	126·60	2·23	80·35	118·73	2·11	4 of 7	0·19	119·54	4·89	0·20	282	67
18R6, 57–67	whole rock	113·74	1·18		not developed (recoil)								
19R1, 63–68	whole rock	115·82	0·96	56·59	115·23	0·96	6 of 12	1·04	115·04	1·42	1·35	309	109
			Weighted mean age:		118·86	1·49							
Hole 1137A													
26R2, 100–105	whole rock	106·08	0·98		not developed (recoil)								
28R4, 13–16	whole rock	110·09	1·05	55·83	107·46	1·05	3 of 9	1·04	107·01	2·19	2·57	333	219
32R7, 52–59	plagioclase	107·43	1·13	93·54	107·07	1·27	7 of 8	1·79	107·25	1·54	1·93	284	31
38R4, 83–88	whole rock	104·57	1·02	37·98	106·94	0·94	5 of 12	1·02	107·27	3·81	1·37	288	80
40R5, 67–74	whole rock	109·58	1·05	57·53	107·53	1·04	5 of 15	1·06	107·65	1·19	1·32	278	84
46R2, 113–121	whole rock	105·15	1·01	40·43	109·45	1·07	5 of 14	2·47	109·27	1·49	3·17	301	32
			Weighted mean age:		107·68	0·47							
Hole 1138A													
80R2, 126–134	plagioclase	112·63	3·03	69·40	100·83	2·94	4 of 8	0·23	102·22	4·28	0·01	275	48
80R2, 126–134	whole rock	98·93	0·91	87·53	100·24	1·09	4 of 7	2·22	100·17	1·66	3·01	294	33
84R5, 88–93	whole rock	99·55	0·95	76·83	100·51	1·00	5 of 7	1·82	101·38	1·39	3·62	141	187
			Weighted mean age:		100·41	0·71							
Hole 1139A													
51R1, 47–52	plagioclase	68·29	0·57	98·53	68·30	0·56	7 of 9	0·57	68·00	0·71	0·18	347	219
52R1, 23–25	whole rock	67·03	0·54	67·09	68·08	0·56	4 of 8	1·56	67·22	1·23	0·02	1018	1045
57R1, 106–111	whole rock	68·54	0·82	98·63	68·44	0·85	7 of 10	2·18	67·57	1·36	0·86	313	633
69R2, 22–24	whole rock	69·49	0·62	83·38	68·62	0·62	9 of 14	1·47	69·34	0·75	1·08	53	228
70R1, 1–10	sanidine	68·50	0·65	93·90	68·32	0·68	6 of 9	2·48	67·86	0·73	0·80	685	309
			Weighted mean age:		68·33	0·29							
Hole 1140A													
31R1, 85–90	plagioclase	35·19	1·40	88·84	33·32	1·40	5 of 8	0·68	32·16	1·68	0·36	325	15
36R3, 79–88	whole rock	37·74	1·12	67·00	34·34	1·22	4 of 7	2·02	35·29	1·72	1·49	277	24
37R3, 26–32	whole rock	38·14	2·78	74·39	34·58	0·76	5 of 7	3·09	32·53	1·24	0·31	308	8
			Weighted mean age:		34·30	0·59							
Hole 1141A													
22R3, 143–150	whole rock	96·87	0·86	87·90	95·17	0·77	5 of 8	0·76	94·89	1·75	1·00	301	36
23R2, 103–107	whole rock	126·26	2·54		not developed (excess^{40}Ar)				93·61	4·04	1·54	328	6
24R2, 27–30	whole rock	141·40	3·81		not developed (excess^{40}Ar)				110·82	16·00	7·14	303	8
			Weighted mean age:		95·17	0·77							
Hole 1142A													
6R1, 12–16	whole rock	93·85	0·78	68·61	94·18	0·83	7 of 13	2·22	93·86	0·82	1·11	360	75
9R3, 91–94	whole rock	89·04	1·46	70·87	94·88	0·90	8 of 12	2·11	95·02	1·24	2·42	294	9
			Weighted mean age:		94.50	0.61							

All ages calculated relative to neutron fluence monitor FCT-3 biotite (28·04 ± 0·12 Ma), decay and abundance constants $\lambda\varepsilon$ = 0·581E–10 yr^{-1}, $\lambda\beta$ = 4·961E–10 yr^{-1}, ^{40}K/K = 1·17E–4, and corrected for ^{37}Ar decay (half-life 35·1 days) and interfering isotopes ^{36}Ar/^{37}Ar[Ca] = 2·64E–4, ^{39}Ar/^{37}Ar[Ca] = 6·73E–4, ^{40}Ar/^{39}Ar[K] = 1·0E–3.

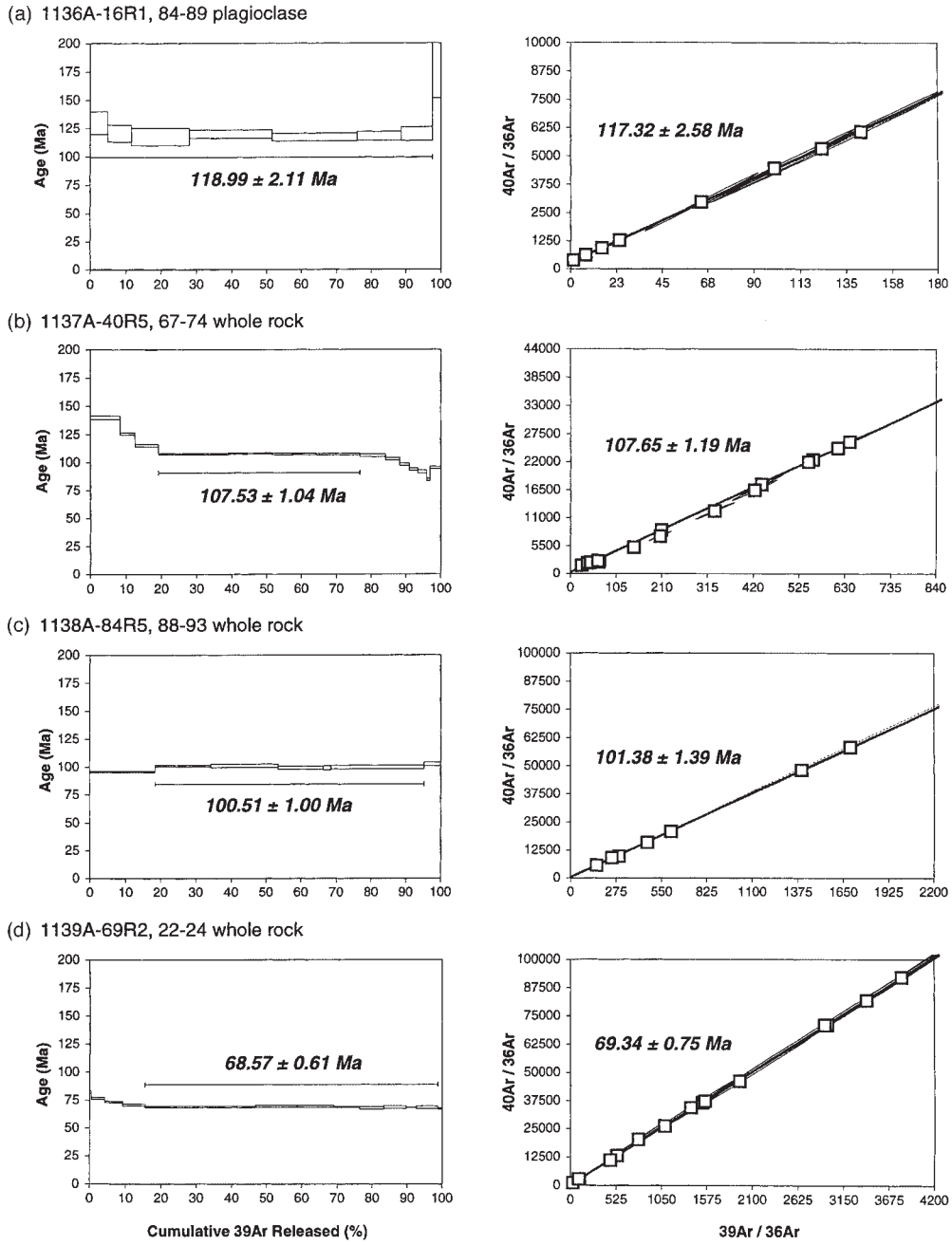

Fig. 2.

polynomial fit to the monitors. Errors in sample J values (0·5%) accumulated from the individual monitor measurements and gradient fitting.

Ar isotopic compositions of samples were measured with a MAP-215/50 mass spectrometer connected to an ultra-high vacuum resistance furnace and Zr–Al getters (Duncan & Hogan, 1994). Samples were heated in 50–100°C increments, from 400°C to fusion. The system is operated in the peak-hopping mode (for m/z = 35, 36, 37, 38, 39, 40) by computer. Peak decay is typically <10% for the MAP system, which has a measured sensitivity of 4×10^{-14} mol/V, and regressed peak heights against time follow linear fits. Mass discrimination on the MAP system was measured using zero-age basalt disks run in the same way as the samples, and was constant at 1·005 (for 2 a.m.u.). The background for the mass spectrometer is $1{\cdot}5 \times 10^{-18}$ mol at $m/z = 36$, 2×10^{-18} mol at $m/z = 39$ and

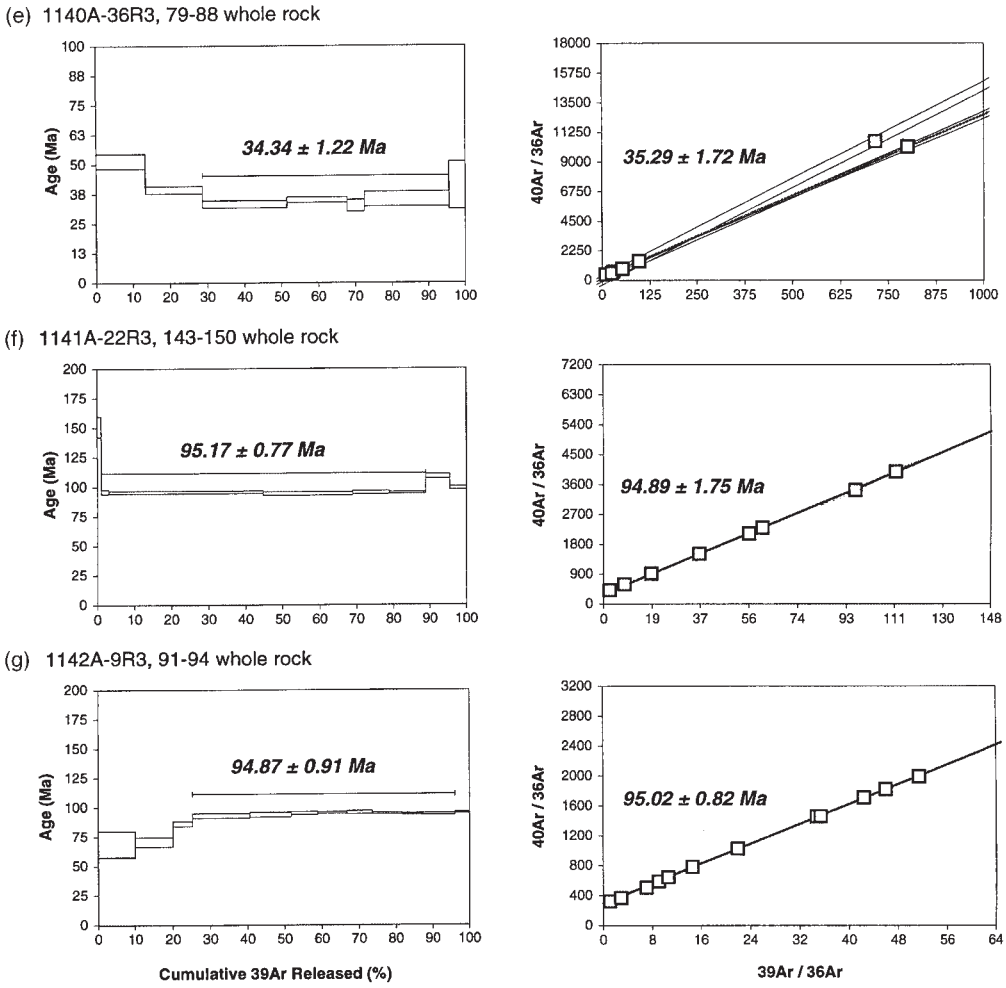

Fig. 2. Representative age spectra (left) and isochron (right) plots for ^{40}Ar–^{39}Ar incremental heating experiments, performed at Oregon State University on ODP Leg 183 feldspars and whole rocks. Open boxes in the age spectra plots show step ages and 2σ analytical uncertainties. Plateau ages (±2σ), indicated by horizontal bar and bold italics, are the weighted means of consecutive, concordant step ages constituting at least 50% of the total gas released during incremental heating experiments. Isochron ages (±2σ) (bold italics) are determined from least-squares regression of isotopic compositions of steps that form the plateaux (□). 2σ errors are generally smaller than the squares, but when larger are plotted as faint ellipses. Calculations based on ArArCALC v21 (Koppers, 2002).

$1{\cdot}5 \times 10^{-16}$ mol at $m/z = 40$. Procedure blanks range from $3{\cdot}0 \times 10^{-18}$ mol ^{36}Ar and $5{\cdot}4 \times 10^{-16}$ mol ^{40}Ar at 600°C to $6{\cdot}4 \times 10^{-18}$ mol ^{36}Ar and $1{\cdot}7 \times 10^{-15}$ mol ^{40}Ar at 1400°C.

NEW RESULTS

Mass spectrometric data are summarized in Table 1, and presented graphically in Fig. 2a–g. Complete experimental data and plots are available in electronic files, which may be downloaded from the *Journal of Petrology* Web site at http://www.petrology.oupjournals.org, or on request from the author. Fitted Ar isotopic ratios from step measurements are used in two ways. Assuming that initial sample Ar compositions were atmospheric (initial $^{40}Ar/^{36}Ar = 295{\cdot}5$) step ages are plotted against cumulative percent ^{39}Ar released, as age spectrum, or plateau diagrams. In addition, isotope correlation diagrams ($^{40}Ar/^{36}Ar$ vs $^{39}Ar/^{36}Ar$) are examined for collinear step compositions whose slope is equivalent to age since closure and whose $^{40}Ar/^{36}Ar$ intercept reveals the initial Ar composition of the system (rock or mineral). We accept an apparent age as an accurate estimate of the sample crystallization age if several statistically testable conditions are met (Dalrymple *et al.*, 1980; Pringle & Duncan, 1995), namely:

(1) a well-defined, mid- to high-temperature plateau is formed by at least three concordant, contiguous steps representing ≥50% of the ^{39}Ar released;

(2) a well-defined isochron exists for the plateau step Ar compositions;

(3) the plateau and isochron ages are concordant;

(4) the isochron $^{40}Ar/^{36}Ar$ intercept is atmospheric composition.

Most whole-rock and all feldspar samples presented in Table 1 meet the criteria listed above. Plateau ages (2σ uncertainties) are the mean of between three and nine step ages, representing $\geq 50\%$ of the total sample ^{39}Ar, weighted by the inverse of variance. Corresponding isochron ages are concordant, although they sometimes have significantly larger uncertainties ($\pm 2\sigma$) because of the small dispersion of very radiogenic step compositions. $^{40}Ar/^{36}Ar$ intercepts are, with a few exceptions, within 2σ uncertainty of the atmospheric value, and these departures are again due to fitting small numbers of closely grouped points in isotope correlation space. A small subset of samples failed to provide acceptable age information, owing to combined effects of Ar loss, excess Ar and Ar recoil, as noted in Table 1 and in the discussion of site ages below. Total gas ages are calculated by recombining all steps from each sample, and are roughly equivalent to conventional K–Ar ages. Results are next evaluated for each site.

SITE 1136

The lowermost sediments at Site 1136 (southern Kerguelen Plateau) are sands and clays of middle to late Albian age (105–107 Ma), biostratigraphically dated from shipboard identification of micro- and nannofossils (Coffin *et al.*, 2000). These are non-marine in part and overlie subaerially erupted basalt flows that are magnetized with normal polarity. Owing to pervasive groundmass alteration to clays, only plagioclase separated from the basalts provided acceptable crystallization ages. Total gas ages range from 114 to 126 Ma, but two plateau ages are more narrowly defined at 118–119 Ma, with individual age uncertainties of ~ 2 Myr. Corresponding isochron ages are concordant, with no evidence of excess Ar problems, but have generally larger age uncertainties. Whole-rock sample 1136-19R-1, 63–68 cm produced an acceptable plateau age of 115·2 Ma, from 57% of the total gas released, and a concordant isochron. However, it lies stratigraphically below the two lava flows dated at 118–119 Ma and cannot, then, be younger. It appears that a small amount of ^{40}Ar has been lost, even from the plateau-forming steps, and this age is not included in the mean. The mean plateau age is $118{\cdot}9 \pm 1{\cdot}5$ Ma (two samples). Figure 2a illustrates one of the two age plateaux, comprising 98% of the total gas released and a concordant isochron, indicating a crystallization age of 118–119 Ma. The normal polarity of magnetization fits with eruption during the earliest part of the long Cretaceous normal chron, as the estimate of the termination of M0r is $\sim 120{\cdot}5$ Ma (Gradstein *et al.*, 1994).

SITE 1137

Campanian (72–76 Ma) sediments overlie the section of subaerially erupted basalt lava flows at Site 1137. All flows are magnetized with normal polarity, consistent with the idea that they may have erupted within the long Cretaceous normal chron (>83 Ma). Total gas ages range from 105 to 110 Ma, whereas plateau ages are more tightly constrained at 107–109 Ma. The whole-rock samples exhibit clear ^{39}Ar and ^{37}Ar recoil effects, in the form of old ages for low-temperature steps and young ages for high-temperature steps, relative to the plateau age (e.g. Fig. 2b). However, unambiguous plateaux and isochrons are present, and the whole-rock ages are confirmed by a plagioclase plateau age with no apparent recoil effects, so it is considered that these are reliable crystallization ages. The mean plateau age is $107{\cdot}7 \pm 0{\cdot}5$ Ma (five samples).

SITE 1138

Upper Cretaceous shallow marine and terrestrial sediments overlie the generally evolved lava flows at Site 1138 in the central Kerguelen Plateau. A well-preserved Turonian–Cenomanian (~ 93 Ma, Gradstein *et al.*, 1994) sequence of glauconitic calcareous sandstone and organic-rich chalks near basement 'thickens to the northeast, suggesting that the basaltic basement rocks could be significantly older than the minimum age indicated by the biostratigraphy' (Coffin *et al.*, 2000). All lava flows are magnetized with normal polarity, indicating eruption in the long Cretaceous normal chron (>83 Ma). Three samples (one plagioclase, two whole rocks) provide a mean plateau age of $100{\cdot}4 \pm 0{\cdot}7$ Ma. An example of acceptable whole-rock plateau and isochron ages is illustrated in Fig. 2c.

SITE 1139

The lowermost sediments at Site 1139 (Skiff Bank, ~ 350 km SW of the Kerguelen Archipelago) are late Eocene–early Oligocene neritic, sandy packstones, probably beach to shallow shelf deposits (Coffin *et al.*, 2000). The volcanic basement here is a subaerially erupted series of alkaline lava flows ranging from trachybasalt to trachyte and rhyolite compositions (Kieffer *et al.*, 2002). The weighted mean plateau age (five samples) is $68{\cdot}3 \pm 0{\cdot}3$ Ma. An example of acceptable whole-rock plateau and isochron ages is illustrated in Fig. 2d.

SITE 1140

Stratigraphic data at this site on the northern edge of the northern Kerguelen Plateau are the most conclusive for determining the age of terminal volcanic activity. This is the only unequivocally submarine eruption site drilled during Leg 183 and, hence, sediments accumulated during and immediately following lava flow formation. The oldest sediments are latest Eocene nannofossil chalks that occur at the top of basement unit 3 (Coffin *et al.*, 2000). Earliest Oligocene (30–34 Ma) nannofossil and foram oozes directly overlie the youngest lava flows (unit 1). Basement unit 1 is magnetized with normal polarity, whereas deeper units 2–6 are reversely magnetized. Combined with the tight biostratigraphic constraint, the magnetic boundary C13n–C13r must occur between basement units 1 and 2. The age of this boundary is currently accepted as 33·6 Ma (Berggren *et al.*, 1995).

Three samples (one plagioclase separate and two whole rocks) have indistinguishable plateau ages that provide a weighted mean age of 34·3 ± 0·6 Ma. Because all samples are from units just below the C13n–C13r boundary, the measured age fits well with stratigraphic data. An example of acceptable whole-rock and isochron ages is illustrated in Fig. 2e.

SITES 1141 AND 1142

These two sites are located within 1 km of each other, on the eastern Broken Ridge, and are considered together for chronological purposes. The lowermost sediments here are middle to late Eocene (35–38 Ma), which is much younger than the upper Cretaceous sediments recovered 350 km to the west at previously drilled ODP Sites 752–755 that did not reach basement. Hence, a major hiatus was expected from shipboard data (Coffin *et al.*, 2000). The basement units (six at each site) are all magnetized with normal polarity.

Some whole-rock samples from Site 1141 exhibited significant amounts of excess ^{40}Ar (mantle derived), as is evident from the total gas ages (Table 1). Hence, for these samples, plateau ages did not develop and isochrons had greater than atmospheric $^{40}Ar/^{36}Ar$ (initial) intercepts. The isochron ages are not precise but are within 2σ analytical uncertainty of the single well-resolved whole-rock age from this site (95·1 ± 0·8 Ma, Fig. 2f). Whole-rock samples from adjacent Site 1142 were better behaved (e.g. Fig. 2g) and produced a mean age of 94·5 ± 0·6 Ma, indistinguishable from the Site 1141 age. The weighted mean age of the three acceptable plateau ages from the combined site analyses is 94·7 ± 0·5 Ma.

DISCUSSION AND CONCLUSIONS

Melt production histories

The new ^{40}Ar–^{39}Ar incremental heating age determinations from drilling sites on the Kerguelen Plateau and Broken Ridge reported here are precise and reproducible because of the generally high K contents (Coffin *et al.*, 2000) and mild alteration of ODP Leg 183 volcanic units selected for dating. The timing of volcanic activity sampled at each site appears to have been brief. A major surprise from this drilling leg is the predominantly subaerial conditions of volcanism encountered at all sites but one (Site 1140). This observation, coupled with the often evolved lava compositions (Coffin *et al.*, 2000), raises the strong possibility that drilling sampled only the final, waning stage of volcanic activity at most locations (Kieffer *et al.*, 2002). The nature and age of underlying basement is unknown, but includes either submarine, flood basalt flows of more primitive compositions, derived from typically large-degree partial melts of the upper mantle as observed at other oceanic LIPs, or remnants of continental lithosphere left behind following dispersion of India from Australia–Antarctica. Coffin *et al.* (2002) have used geophysical data (seismic reflection, gravity) to distinguish continental basement from oceanic crust, so as to calculate melt volumes used to estimate magma production rates throughout the history of the Kerguelen hotspot.

The new ages from Site 1136 (118–119 Ma) are the oldest yet measured for the Kerguelen Plateau and are approximately contemporaneous with the most reliable ages from the Rajmahal basalts, eastern India (Baksi, 1995; Coffin *et al.*, 2002; Kent *et al.*, 2002). Most of these lava flow compositions are tholeiitic, reflecting rather large degrees of mantle melting, and similar in composition to those recovered at other southern Kerguelen Plateau sites (738, 749, 750) (Coffin *et al.*, 2000). Coffin *et al.* (2002) have noted that there is both geochemical and geophysical evidence for continental crust beneath parts of the southern Kerguelen Plateau (Operto & Charvis, 1996; Frey *et al.*, 2002), whereas other parts are totally oceanic. A prominent negative free-air gravity lineament just south of Site 747 (Fig. 1) is the physiographic basis for dividing the southern from the central Kerguelen Plateau (Coffin *et al.*, 2002). We concur with Coffin *et al.* (2002) in assuming that all oceanic crust in the southern Kerguelen Plateau was formed between 120 and 110 Ma, but probably more narrowly focused in the range of the most reliable age determinations, 119–118 Ma, and contiguous with contemporaneous volcanism in eastern India at the Rajmahal basalts, 118–116 Ma.

Reliable basement ages for the central Kerguelen Plateau come from Site 1138 (100–101 Ma). The ~85 Ma age for Site 747 (Pringle *et al.*, 1997) does not meet the

minimum requirements for an acceptable crystallization age. The eastern Broken Ridge (Site 1141–1142) is slightly younger (95 Ma) and, on reconstruction to pre-Southeast Indian Ridge geometry, lay adjacent to the central Kerguelen Plateau (see Coffin *et al.*, 2002, fig. 4). Given the geochemical evidence for continental crust involvement in the petrogenesis of basalt compositions at several central Kerguelen Plateau sites (Coffin *et al.*, 2000; Neal *et al.*, 2002) and the possibility that older basement underlies these sites, it is not clear how to apportion volumes to time periods for this region of the province. A similar uncertainty exists for Sites 1139 and 1140 on the northern Kerguelen Plateau. Coffin *et al.* (2002) have assumed that measured ages at the surface of the plateau are regionally and vertically representative of the entire anomalously thick crust. An equally plausible, alternative possibility is that a much larger area of the province was built initially, at the time of the southern Kerguelen Plateau, but this older foundation has been covered progressively northward by slow southward plate motion over the Kerguelen hotspot. The northward age progression from Site 750 (112–110 Ma) to Site 1137 (108–109 Ma), Site 1138 (101–100 Ma) and Site 1141–1142 (94–95 Ma) is consistent with plate reconstructions in the southern Indian Ocean for this time frame (Coffin *et al.*, 2002, fig. 4). This overprinting mechanism is clearly the explanation for Site 1139 (Skiff Bank) and the young volcanism at Heard and McDonald Islands and seamounts trending toward the Kerguelen Archipelago. An unknown portion of the northern Kerguelen Plateau existed before the Archipelago began construction at ~40 Ma. It is unlikely that a large portion of this region was built with the southern Kerguelen Plateau because of the limited space in the narrow ocean basin between India and Antarctica at that time (~118 Ma), but some portions could be contemporaneous with parts of the Ninetyeast Ridge (80–38 Ma, Duncan, 1991).

Caution should be used, then, in evaluating dynamic models of plume flow and melting history with the new chronological database for the Kerguelen hotspot. The distribution of surficial ages across the Kerguelen Plateau, making the assumption of uniform crustal age beneath, appears to support a much more protracted history of high (but not extraordinary) melt production rates over perhaps 30 Myr. This history may be difficult to reconcile with the start-up plume head dynamic models that are proposed to account for the widespread but very brief volcanic distributions in other LIPs (e.g. Storey *et al.*, 1996; Duncan *et al.*, 1997). Partitioning most of the crust underlying the central and some under the northern Kerguelen Plateau into the earliest volcanic activity (118–119 Ma), however, gives a melt production history very similar to that of other well-documented LIPs. Only deep drilling combined with additional multichannel seismic reflection will convincingly resolve these two scenarios.

Sr isotopic composition of seawater

The seawater Sr isotopic evolution curve (Howarth & McArthur, 1997) exhibits a decline between ~122 and ~112 Ma, reflecting extraordinary contributions of relatively unradiogenic Sr from hydrothermal activity, as noted by Ingram *et al.* (1994). Because Sr in the ocean has a residence time of ~3 Myr, the high hydrothermal input must have waned at ~115 Ma for the seawater Sr isotopic composition to rebound by 112 Ma. This input, of course, could have come from increased sea-floor spreading or construction of ocean plateaux (e.g. Ontong Java, Kerguelen). But the increase in radiogenic Sr in seawater after ~115 Ma means that there is no evidence for significant submarine eruptions at the Kerguelen Plateau (or elsewhere) from this time until ~93 Ma, the next abrupt decrease in the Sr isotopic evolution curve. Hence the Sr isotopic curve for seawater supports the idea that most of the submarine Kerguelen Plateau volcanic activity occurred in the period 115–119 Ma.

Global anoxic events

With regard to the timing of environmental crises, the global anoxic event OAE1 (the 'Selli' black shale) occurred in early Aptian time, just after magnetic anomaly M0r (~120 Ma, Gradstein *et al.*, 1994). Although the vast and totally submarine Ontong Java Plateau, much of which was formed at 121 ± 1 Ma (Mahoney *et al.*, 1993; Tejada *et al.*, 1996, 2002), has been implicated in altering seawater compositions through hydrothermal activity (Bralower *et al.*, 1997; Sinton & Duncan, 1997), the rapid submarine construction of the southern Kerguelen Plateau by 118–119 Ma may have contributed to this global oceanographic change. Global anoxic event OAE2 (the 'Bonarelli' black shale) occurred very near the boundary between Cenomanian and Turonian time (~93·5 Ma, Gradstein *et al.*, 1994). It appears certain that some portion of the Kerguelen hotspot track, probably the northernmost Ninetyeast Ridge now buried beneath the Bengal Fan, was active at this time, but eruption rates were nothing close to those responsible for Ontong Java Plateau and southern Kerguelen Plateau volcanism, and it is unlikely that the Kerguelen hotspot can be linked to the OAE2 event. Instead, Caribbean Plateau construction has been proposed as the agent of the OAE2 crisis (Sinton & Duncan, 1997).

ACKNOWLEDGEMENTS

We thank the officers and crew of the R.V. *JOIDES Resolution* for their technical mastery and good humor in

obtaining drill cores, John Huard for assistance with sample preparation and mass spectrometric analyses at OSU, and Anthony Koppers, Ian McDougall and an anonymous reviewer for their comments that improved the paper. Malcolm Pringle collaborated in sampling, sharing unpublished radiometric data from his laboratory, and discussions of the volcanic history of this hotspot system. R.A.D. was supported by the JOI/USSSP to participate in the Ocean Drilling Program.

REFERENCES

Baksi, A. K. (1995). Petrogenesis and timing of volcanism in the Rajmahal flood basalt province, northeastern India. *Chemical Geology* **121**, 73–90.

Barling, J., Goldstein, S. L. & Nicholls, I. A. (1994). Geochemistry of Heard Island (Southern Indian Ocean): characterization of an enriched mantle component and implications for enrichment of the sub-Indian Ocean mantle. *Journal of Petrology* **35**, 1017–1053.

Barron, J. & Larsen, B. (eds) (1989). *Proceedings of the Ocean Drilling Program, Initial Reports*, 119. College Station, TX: Ocean Drilling Program.

Berggren, W. A., Kent, D. V., Swisher, C. C., III & Aubry, M.-P. (1995). A revised Cenozoic geochronology and chronostratigraphy. In: Berggren, W. A., Kent, D. V. & Hardenbol, J. (eds) *Geochronology, Time Scales and Global Stratigraphic Correlation. Society of Economic Paleontologists and Mineralogists, Special Publication* **54**, 129–212.

Bralower, T. J., Fullagar, P. D., Paull, C. K., Dwyer, G. S. & Leckie, R. M. (1997). Mid-Cretaceous strontium-isotope stratigraphy of deep-sea sections. *Geological Society of America Bulletin* **109**, 1421–1442.

Campbell, I. H. & Griffiths, R. W. (1990). Implications of mantle plume structure for the evolution of flood basalts. *Earth and Planetary Science Letters* **99**, 79–93.

Coffin, M. F., Frey, F. A., Wallace, P. J., *et al.* (eds) (2000). *Proceedings of the Ocean Drilling Program, Initial Reports*, 183. College Station, TX: Ocean Drilling Program (CD-ROM).

Coffin, M. F., Pringle, M. S., Duncan, R. A., Gladczenko, T. P., Storey, M., Müller, R. D. & Gahagan, L. A. (2002). Kerguelen hotspot magma output since 130 Ma. *Journal of Petrology* **43**, 1121–1139.

Dalrymple, G. B., Lanphere, M. A. & Clague, D. A. (1980). Conventional and $^{40}Ar/^{39}Ar$ K–Ar ages of volcanic rocks from Ojin (Site 430), Nintoku (Site 432), and Suiko (Site 433) Seamounts and the chronology of volcanic propagation along the Hawaiian–Emperor Chain. In: Jackson, E. D., Koisumi, T. *et al.* (eds) *Initial Reports of the Deep Sea Drilling Project*, 55. Washington, DC: US Government Printing Office, pp. 659–676.

Dalrymple, G. B., Alexander, E. C., Jr, Lanphere, M. A. & Kraker, G. P. (1981). Irradiation of samples for $^{40}Ar/^{39}Ar$ dating using the Geological Survey TRIGA reactor. *US Geological Survey Professional Paper* **1176**, 55 pp.

Duncan, R. A. (1991). Age distribution of volcanism along aseismic ridges in the eastern Indian Ocean. In: Weissel, J., Peirce, J., Taylor, E., Alt, J., *et al.* (eds) *Proceedings of the Ocean Drilling Program, Scientific Results*, 121. College Station, TX: Ocean Drilling Program, pp. 507–517.

Duncan, R. A. & Hogan, L. G. (1994). Radiometric dating of young MORB using the ^{40}Ar–^{39}Ar incremental heating method. *Geophysical Research Letters* **21**, 1927–1930.

Duncan, R. A., Hooper, P. R., Rehacek, J., Marsh, J. S. & Duncan, A. R. (1997). The timing and duration of the Karoo igneous event, southern Gondwana. *Journal of Geophysical Research* **102**, 18127–18138.

Erba, E. (1994). Nannofossils and superplumes: the early Aptian 'nannoconid crisis'. *Paleoceanography* **9**, 483–501.

Frey, F. A., Weis, D., Borisova, A. & Xu, G. (2002). Involvement of continental crust in the formation of the Cretaceous Kerguelen Plateau: new perspectives from ODP Leg 120 sites. *Journal of Petrology* **43**, 1207–1239.

Frohlich, F. & Wicquart, E. (1989). Upper Cretaceous and Paleocene sediments from the northern Kerguelen Plateau. *Geo-Marine Letters* **9**, 127–133.

Gradstein, F. M., Agterberg, F. P., Ogg, J. G., Hardenbol, J., van Geen, P., Thierry, J. & Huang, Z. (1994). A Mesozoic time scale. *Journal of Geophysical Research* **99**, 24051–24074.

Howarth, R. J. & McArthur, J. M. (1997). Statistics for strontium isotope stratigraphy: a robust LOWESS fit to the marine Sr-isotope curve for 0 to 206 Ma, with look-up table for derivation of numeric age. *Journal of Geology* **105**, 441–456.

Ingram, B. L., Coccioni, R., Montanari, A. & Richter, F. M. (1994). Strontium isotopic composition of mid-Cretaceous seawater. *Science* **264**, 546–550.

Kent, R. W., Storey, M. S. & Saunders, A. D. (1992). Large igneous provinces: sites of plume impact or incubation? *Geology* **20**, 891–894.

Kent, R. W., Pringle, M. S., Müller, R. D., Saunders, A. D. & Ghose, N. C. (2002). $^{40}Ar/^{39}Ar$ geochronology of the Rajmahal basalts, India, and their relationship to the Kerguelen Plateau. *Journal of Petrology* **43**, 1141–1153.

Kieffer, B., Arndt, N. T. & Weis, D. (2002). A bimodal alkalic shield volcano on Skiff Bank: its place in the evolution of the Kerguelen Plateau. *Journal of Petrology* **43**, 1259–1286.

Koppers, A. A. P. (2002). ArArCALC—software for $^{40}Ar/^{39}Ar$ age calculations. *Computers in Geosciences* (in press).

Leclaire, L., Bassias, Y., Denis-Clochiatti, M., Davies, H. L., Gautier, I., Gensous, B., Giannesini, P.-J., Patriat, P., Segoufin, J., Tesson, M. & Wannesson, J. (1987). Lower Cretaceous basalt and sediments from the Kerguelen Plateau. *Geo-Marine Letters* **7**, 169–176.

Mahoney, J. J., Storey, M. S., Duncan, R. A., Spencer, K. J. & Pringle, M. S. (1993). Geochemistry and age of the Ontong Java Plateau. In: Pringle, M. S., *et al.* (eds) *The Mesozoic Pacific: Geology, Tectonics and Volcanism. Geophysical Monograph, American Geophysical Union* **77**, 233–262.

McDougall, I. & Harrison, T. M. (1999). *Geochronology and Thermochronology by the $^{40}Ar/^{39}Ar$ Method*, 2nd edn. New York: Oxford University Press.

Neal, C. R., Mahoney, J. J. & Chazey, W. J., III (2002). Mantle sources and the highly variable role of continental lithosphere in basalt petrogenesis of the Kerguelen Plateau and Broken Ridge LIP: results from ODP Leg 183. *Journal of Petrology* **43**, 1177–1205.

Nicolaysen, K., Frey, F. A., Hodges, K., Weis, D., Giret, A. & Leyrit, H. (2000). $^{40}Ar/^{39}Ar$ geochronology of flood basalts from the Kerguelen Archipelago, southern Indian Ocean: implication for Cenozoic eruption rates of the Kerguelen plume. *Earth and Planetary Science Letters* **174**, 313–328.

Operto, S. & Charvis, P. (1996). Deep structure of the southern Kerguelen Plateau (southern Indian Ocean) from ocean bottom seismometer wide-angle seismic data. *Journal of Geophysical Research* **101**, 25077–25103.

Pringle, M. S. & Duncan, R. A. (1995). Radiometric ages of basement lavas recovered at Loen, Wodejebato, MIT, and Takuyo–Daisan Guyots, northwestern Pacific Ocean. In: Haggerty, J. A., Premoli-Silva, I., *et al.* (eds) *Proceedings of the Ocean Drilling Program, Scientific Results*, 144. College Station, TX: Ocean Drilling Program, pp. 547–557.

Pringle, M. S., Coffin, M. F. & Storey, M. S. (1997). Estimated melt production of the Kerguelen hot spot. *EOS Transactions, American Geophysical Union* **78**, 728.

Renne, P. R., Deino, A. L., Walter, R. C., Turrin, B. D., Swisher, C. C., Becker, T. A., Curtis, G. H., Sharp, W. D. & Jaouni, A.-R. (1994). Intercalibration of astronomical and radioisotopic time. *Geology* **22**, 783–786.

Richards, M. A., Duncan, R. A. & Courtillot, V. (1989). Flood basalts and hotspot tracks: plume heads and tails. *Science* **246**, 103–107.

Royer, J.-Y. & Coffin, M. F. (1992). Jurassic to Eocene plate reconstructions in the Kerguelen Plateau region. In: Wise, S. W., Jr, Schlich, R., *et al.* (eds) *Proceedings of the Ocean Drilling Program, Scientific Results*, 120. College Station, TX: Ocean Drilling Program, pp. 763–776.

Schlich, R. & Wise, S. W., Jr (eds) (1989). *Proceedings of the Ocean Drilling Program, Initial Reports*, 120. College Station, TX: Ocean Drilling Program.

Sinton, C. W. & Duncan, R. A. (1997). Potential links between ocean plateau volcanism and global anoxia at the Cenomanian–Turonian boundary. *Economic Geology* **92**, 836–842.

Storey, M., Duncan, R. A., Larsen, H. C., Pedersen, A. K., Waagstein, R., Larsen, L. M., Tegner, C. & Lesher, C. A. (1996). Impact and rapid flow of the Iceland plume beneath Greenland at 61 Ma. *EOS Transactions, American Geophysical Union* **77**, 839.

Tejada, M. L. G., Mahoney, J. J., Duncan, R. A. & Hawkins, M. P. (1996). Age and geochemistry of basement and alkalic rocks of Malaita and Santa Isabel, Solomon Islands, southern margin of Ontong Java Plateau. *Journal of Petrology* **37**, 361–394.

Tejada, M. L. G., Mahoney, J. J., Neal, C. R., Duncan, R. A. & Petterson, M. G. (2002). Basement geochemistry and geochronology of central Malaita, Solomon Islands, with implications for the origin and evolution of the Ontong Java Plateau. *Journal of Petrology* **43**, 449–484.

Weis, D., Frey, F. A., Schlich, R., Schaming, M., Montigny, R., Damasceno, D., Mattielli, N., Nicolaysen, K. E. & Scoates, J. S. (2002). Trace of the Kerguelen mantle plume: evidence from seamounts between the Kerguelen Archipelago and Heard Island, Indian Ocean. *G-Cubed—Geology, Geochemistry & Geophysics*, in press.

Whitechurch, H., Montigny, R., Sevigny, J., Storey, M. & Salters, V. J. M. (1992). K–Ar and $^{40}Ar/^{39}Ar$ ages of central Kerguelen Plateau basalts. In: Wise, S. W., Jr, Schlich, R., *et al.* (eds) *Proceedings of the Ocean Drilling Program, Scientific Results*, 120. College Station, TX: Ocean Drilling Program, pp. 71–77.